Desalination and Water Treatment
www.deswater.com

doi: 10.5004/dwt.2021.27352

228 (2021) 286–296
July

Magnetic solid-phase extraction of Cd(II) from water samples using magnetic nanoparticles impregnated walnut shells powder (MNP_S-WSP)

Mansoor Khan[a,*], Shaista Naseer[a], Muslim Khan[a], Ruqia Nazir[a], Amir Badshah[a], Adnan[b], Shaukat Shujah[a], Asia Parveen[a]

[a]*Department of Chemistry, Kohat University of Science and Technology, Kohat, KPK-Pakistan, emails: mansoor009988@gmail.com (M. Khan), shaistakhan099@yahoo.com (S. Naseer), unigraz2012@yahoo.com (M. Khan), ruqianazir@yahoo.com (R. Nazir), amirqau@yahoo.com (A. Badshah), shaukat-shujah@yahoo.com (S. Shujah)*
[b]*Institute of Chemical Sciences, University of Swat, 19130, KPK-Pakistan, email: adnanchem@uswat.edu.pk*

Received 15 December 2020; Accepted 20 April 2021

ABSTRACT

In the present study synthesis of magnetic nanoparticle (MNPs), impregnated walnut shell powder (MNPs-WSP) were carried out using the co-precipitation method and used for the solid-phase extraction of Cd(II) from environmental water samples. Impregnated walnut shell powder (MNPs-WSP) was characterized by using Fourier transform infrared spectroscopy for functional group, scanning electron microscopy for surface morphology, energy dispersive X-ray analysis for elemental analysis, X-ray diffraction for crystallinity and SAA for surface area, pore volume and pore size. For quantitative percent recovery various analytical parameters like solution pH, sample volume, vertex time, temperature and initial metal ion concentration were optimized. Analytical parameters like limit of detection, limit of quantification and enhancement factor were also calculated under optimized experimental conditions. The kinetic data shows that the adsorption of Cd(II) on MNPs and MNPs-WSP follows pseudo-second-order kinetics. Values of $\Delta H°$, $\Delta S°$ and $\Delta G°$ show that these adsorption processes are endothermic and feasible in nature. For equilibrium studies different isotherms like Langmuir and Freundlich, adsorption isotherms were applied. The method was successfully applied to environmental water samples like tap water, underground water, dam water and wastewater with satisfied recovery results.

Keywords: Solid phase extraction; Magnetic nanoparticle; Co-precipitation; Preconcentration

1. Introduction

Heavy metals are elements having atomic weights between 63.5 and 200.6 amu, and a specific gravity greater than 5.0. With the rapid development of industries such as metal plating facilities, mining operations, fertilizer industries, tanneries, batteries, paper industries and pesticides, etc., heavy metals wastewaters are directly or indirectly discharged into water bodies to cause environmental water pollution [1,2]. Unlike organic contaminants, heavy metals are non-biodegradable and tend to accumulate in living tissues and cause many harmful effects [3]. Industrial wastewaters mostly include different toxic metals such as zinc, copper, nickel, mercury, cadmium, lead and chromium, etc. [4].

Among these heavy metals, cadmium (Cd) is an important heavy metal and widely known as a hazardous environmental contaminant. It was reported that excessive exposure of Cd can cause severe diseases, including liver and kidney diseases in human beings [5]. According to International Agency for Research on Cancer cadmium is carcinogenic and also causes chromosomal aberration [6]. The accurate determination of

* Corresponding author.

trace concentrations of metal ions in manmade and natural water resources is very complex. The direct determination of extremely low concentrations of the required elements by modern atomic spectroscopic methods, such as atomic absorption spectrometry (AAS) and inductively coupled plasma atomic emission spectrometry/mass spectrometry (ICP-AES/MS), is often difficult. The limitations are not only associated with the insufficient sensitivity of these techniques but also with matrix interference. For this reason, preconcentration of trace elements from the matrix is often required [7–9].

In the literature, various methods used for the preconcentration of heavy metal such as solid-phase extraction [10,11], co-precipitation [12], chemical precipitation, coagulation, membrane synthesis [13] and various liquid–liquid extraction techniques such as dispersive liquid–liquid extraction, supramolecular solvent base liquid-phase extraction and headspace liquid phase micro extraction have been extensively used by researchers in the recent past [14,15]. Due to high consumption of organic compounds, matrix interferences and low sensitivity in liquid–liquid extraction make it more expensive and also not environmental friendly [16].

As compared to other extraction techniques, solid-phase extraction has significant advantages like low running cost, high recovery, selectivity, short extraction time and low consumption of organic compound [17,18]. Therefore, solid-phase extraction is a better choice for the extraction of heavy metals from environmental samples [19].

The selection of appropriate sorbent/adsorbent is an important strategy in SPE to develop an analytical procedure [2]. Different researchers used different adsorbents for the removal of heavy metals such as activated coconut shell carbon [20], mango peel waste [21], sawdust [22], silica gel [23], chelating resins [8], modified ZrO_2, amberlite and fullerene [24] have been employed in SPE.

In the last few decades' nanotechnology has attracted great intention of the scientist due to its unique properties [25]. The nanometer size particles are 1 to 100 nm in diameter, having large surface area, large surface-to-volume ratio and thus having large adsorption capacity [26,27].

Till date, several magnetic nanomaterials, including maghaemite nanoparticles [28], Fe_3O_4 magnetic nanoparticles [29], Fe_3O_4 nanoparticles functionalized and stabilized with compounds like humic acid [30], amino-functionalized polyacrylic acid [31], orange peel modified with MNPs [3], and various biopolymers like gum Arabic [32], and polysaccharides [33] have been used as adsorbents for the removal of metal ions from aqueous solution.

The objective of the present work was to develop, a magnetic nano-adsorbent (MNPs–WSP) by the surface modification of Fe_3O_4 nanoparticles (MNPs) with walnut shells powder (WSP) with the aim of exploring its feasibility as an adsorbent for the removal of cadmium taken as a model toxic metal ion.

2. Materials and methods

2.1. Reagents

All chemicals used were of analytical reagent grade or similar purity. Cadmium nitrate hexahydrate [$Cd(NO_3)_2{\cdot}6H_2O$], ferric chloride hexahydrate ($FeCl_3{\cdot}6H_2O$), and ferrous sulfate heptahydrate ($FeSO_4{\cdot}7H_2O$), ammonia solution (25%), hydrochloric acid (37%), sodium hydroxide, phosphoric acid, and acetic acid were supplied by departmental laboratories and all these chemicals purchased from Sigma Aldrich and Merck KGaA, Dramstadt, Germany.

2.2. Instruments

A Perkin-Elmer flame atomic absorption spectrometer Model AA 200 having (air–acetylene flame, 10 cm long-slot burner head and hollow cathode lamp was used as radiation source) was used for absorbing measurement of the entire Cd(II) samples. The selected wavelength for the determination of cadmium was 228.78 nm. The measurements were performed with the continuous aspiration mode of FAAS. A pH-meter with a glass electrode of model (422-WTW, Weilheim) was used for pH measurements. The solid phase was separated by using an Nd magnet. Vortex mixer (Wiggen Hauser, Malaysia) was used for homogenous mixing of solutions.

FT-IR spectra of the adsorbent were carried by using IR Prestigue-21 SHIMADZU HK in the range of 4,000–500 cm^{-1}. For surface morphology of the adsorbent, the scanning electron microscopy (SEM) images were obtained by using 30 KV SEM and energy dispersive X-ray analysis (EDX; JSM5910, JEOL, Japan). The surface area, pore volume and pore width of adsorbent were determined by the BET-N_2 method using a surface area analyzer NOVA Quantachrome USA.

2.3. Preparation of MNPs and MNP-WSP

For the preparation of MNPs salts of Fe^{2+} and Fe^{3+} were mixed in 1:2 ratios in alkaline media for precipitation. For this purpose, 6.3 g of $FeCl_3{\cdot}6H_2O$ and 4.2 g $FeSO_4 7H_2O$ were dissolved in 200 mL of distilled water with vigorous stirring under nitrogen atmosphere. The solution was kept at 80°C; black precipitate of MNPs was obtained when 20 mL of 25% ammonia solution was added. The Fe_3O_4 obtained was washed twice with distilled water and dried in an oven at 100°C [34–36].

$$Fe_3SO_4 \cdot 7H_2O + 2FeCl_3 \cdot 6H_2O + 8NH_4OH \rightarrow Fe_3O_4 + 6NH_4Cl + \left(NH_4\right)_2 SO_4 + 17H_2O \quad (1)$$

Walnut shells were collected commercially, washed with distilled water, and dried it in sunlight. The dried WS were grinded in a grinder and passed through a sieve to obtain a uniform particle size of 355 μm. Walnut shell powders were washed several times with distilled water and ethanol in order to completely remove the dust particles. For the impregnation of MNPs on WSP, 5.0 g of WSP was added to the solution of MNPs at 80°C for 120 min under vigorous stirring. The resultant MNPs-WSP was filtered, washed twice with distilled water and dried in oven at 100°C. The MNPs-WSP obtained was checked for its magnetic property with a magnetic rod [37].

2.4. Application of the proposed solid phase extraction method

The proposed solid phase extraction method was applied to four real water samples like tap water of our research laboratory, dam water of Zibi dam Karak, underground water of Karak and wastewater of Janana mill of Kohat for additional recovery. All the real water samples were passed through a cellulose membrane filter having 0.45 μm pore size (Millipore) prior to solid-phase extraction experiments to remove the solid suspended particles.

2.5. Adsorption

Batch experiments were carried for the adsorption process of Cd(II). Batch adsorption studies were carried out in 50 mL of centrifuge tubes, which contain 10 μg mL^{-1} Cd(II) solutions at pH 7. The sample solutions were then added to another tube contain 0.1 g of MNPs-WSP, MNPs and WSP as adsorbent and the solutions were allowed for 4 min under the influence of vortex having a vortex speed of 1,400 rpm. After complete adsorption, MNPs-WSP and MNPs were separated by using an external magnetic field, the liquid phase was separated using a pipette and WSP was separated by filtration and the residual concentrations of Cd(II) in the filtrates were determined by atomic absorption spectrophotometer with air-acetylene flame.

Adsorption capacity (q_e) of Cd(II) and percent adsorption was calculated according to the following general equations:

$$\text{Adsorption capacity } q_e = \frac{\left(C_i - C_f\right)}{m} V \tag{2}$$

$$\%\ \text{adsorption} = \frac{\left(C_i - C_f\right)}{C_i} \times 100 \tag{3}$$

where q_e is the amount of Cd(II) adsorbed on the adsorbent (mg g^{-1}), C_i represents the initial concentration of Cd(II) added before equilibration and C_f represents equilibrium concentrations of Cd(II), V is the volume of Cd(II) solution (mL) and m is the amount of adsorbent (g).

2.6. Desorption

For quantitative recoveries of analyte, 5 mL of 0.1 M of HCl in acetone was added to the adsorbent. The solid phase was again subjected to vortex for 4 min and again separated using external magnetic field for MNPs-WSP and MNPs and filter paper for WSP. Acetone in eluent was evaporated on a water bath and 100 μL of eluent were injected into the nebulizer of the FAAS by using the micro injection system for the measurement of concentration. Adsorption capacity and % adsorption of Cd(II) on MNPs-WSP, MNPs and WSP were calculated using Eqs. (1) and (2).

3. Result and discussion

3.1. Characterization of adsorbent

The adsorbent impregnated walnut shell powder (MNPs-WSP) was characterized by using Fourier transform infrared spectroscopy, SEM, EDX, SAA and X-ray diffraction (XRD). The FT-IR spectra for WSP are presented in Fig. 1a in the wavenumber range of 4,000–500 cm^{-1}. It can be seen in Fig. 1a, that the biomaterial has different functional groups. The broadband at 3,327 cm^{-1} corresponds to –OH stretching vibration of the hydroxyl groups. These groups could interfere with the metal uptake and bond formation with the magnetic nanoparticles. The binding of magnetic nanoparticles onto the WSP surface was confirmed by FT-IR spectrum shown in Fig. 1b. It can be seen in Fig. 1b that the adsorption band for the Fe–O is appeared at 548 cm^{-1}. This peak is characteristic for MNPs. The strong absorption band in FT-IR spectra (Fig. 1b) at 3,334 cm^{-1} corresponds to Fe–OH stretching that also confirms that the impregnation of WSP surface with MNPs.

The physical nature and surface morphology of MNPs-WSP, MNPs and WSP can be viewed from the SEM micrograph given in Fig. 2. SEM micrographs of the three adsorbents present the morphological characteristics favorable for metal adsorption. Fig. 2a shows the heterogeneous, porous surface morphology of WSP having a mean particle diameter of 0.11 μm. Fig. 2b shows a spherical morphology of MNPs with a particle size of 500 nm and Fig. 2c. More spherical and dispersed nature shows morphology of MNPs-WSP similar to those of MNPs but with a much smoother surface. The more spherical and dispersed nature of MNPs-WSP (Fig. 2c) as compared to MNPs and WSP (Fig. 2a and b) can be seen from the SEM micrograph.

Elemental analysis of MNPs, MNPs-WSP and WSP can be determined by analyzing the EDX mapping (shown in Fig. 3). High concentration of Fe in MNPs (Fig. 3a) and

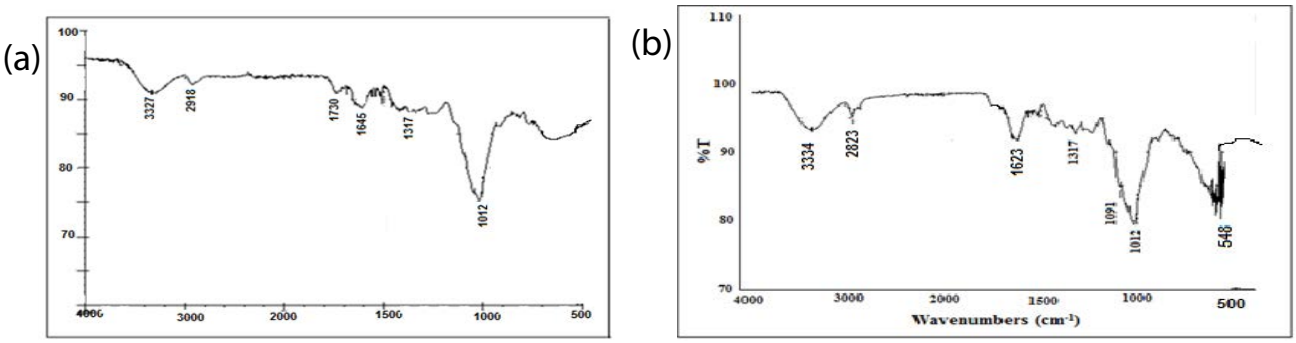

Fig. 1. FT–IR spectra of WSP (a) and MNPs-WSP (b) for surface functional group.

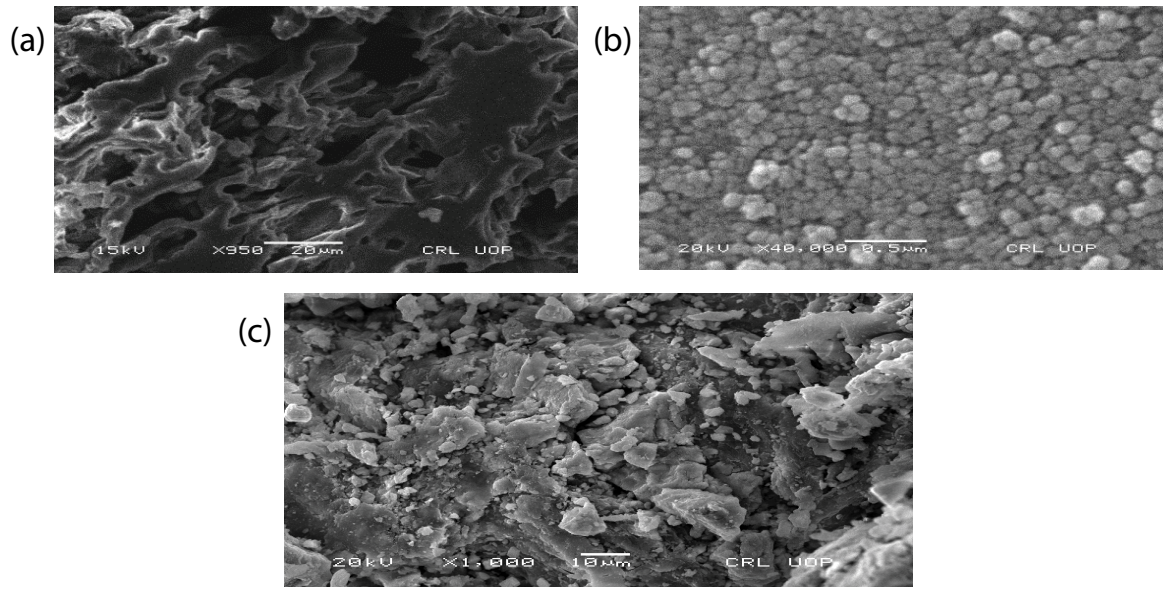

Fig. 2. SEM images of MNPs-WSP, MNPs and WSP for surface morphology.

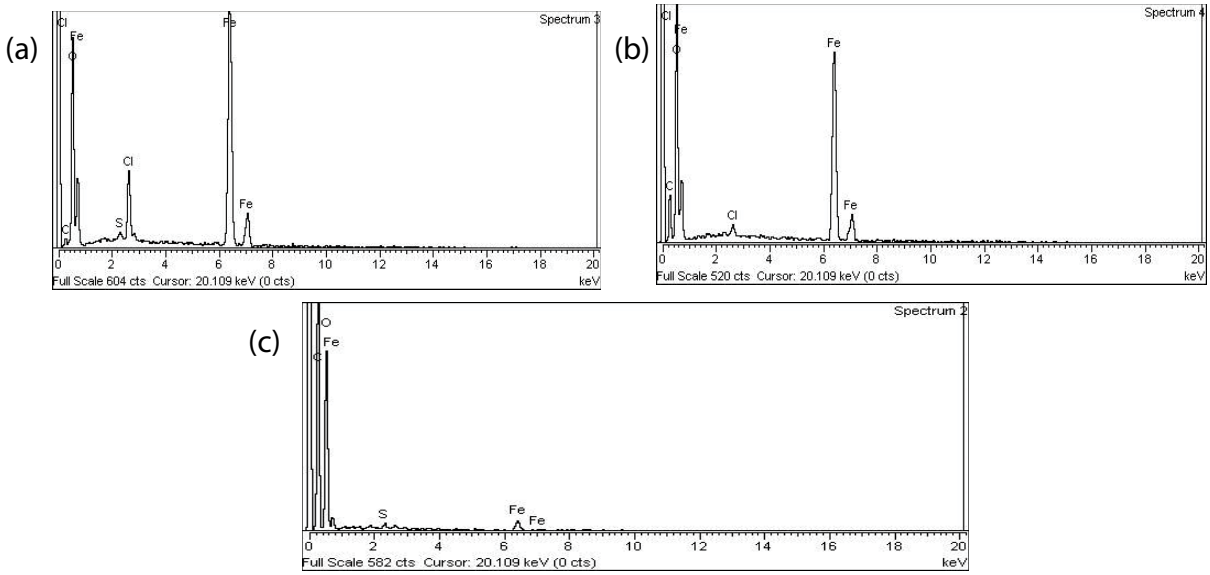

Fig. 3. EDX mapping of MNPs (a), MNPs-WSP (b) and WSP (c).

MNPs-WSP (Fig. 3b) confirm the impregnation of MNPs on the surface of WSP. Fe concentration is almost negligible in the case of WSP (Fig. 3c).

The process of N_2 adsorption/desorption has been used for the surface area of Brunauer, Emmett, Teller (BET) and Barrett, Joyner, Hallenda (BJH), pore volume and pore size of adsorbents (MNP, MNPs-WSP, and WSP). Results are given in Table 1. It was concluded from Table 1 that after modification with MNP, the BET surface area of WSP increased from 38.12 to 55.21 $mg^2\ g^{-1}$. There is also increased observed in case of pore volume and pore size from 0.14 to 0.17 cc g^{-1} and 132.5 to 137.2 Å respectively.

XRD is an effective characterization to validate the crystal structure of adsorbents. The XRD patterns for

Table 1
Surface area, pore volume and pore size of MNPs, MNPs-WSP and WSP by BET and BJH methods

Adsorbents	Method	Surface area ($mg^2\ g^{-1}$)	Pore volume (cc g^{-1})	Pore size (Å)
MNP	BET	81.14	0.26	45.23
	BJH	105.43		
MNP-WSP	BET	55.21	0.17	137.2
	BJH	64.88		
WSP	BET	38.12	0.14	132.5
	BJH	49.2		

impregnated walnut shells powder (MNP-WSP), walnut shells powder (WSP) and magnetic nanoparticles (MNP) are shown in Fig. 4. It is obvious that due to impregnation of magnetic nanoparticles on surface of walnut shell powder makes it magnetic. XRD pattern shown in Fig. 4 indicates the 2θ peak at 35.5° that corresponds to impregnated walnut shells powder (MNP-WSP). While in case of WSP no 2θ peak observed which shows the amorphous nature of walnut shells powder. XRD pattern of MNPs gives characteristic peak at 35.5° attributed to the crystal plane of magnetite at 311 which is matched well with the standard XRD data of the Fe_3O_4 from Joint committee on powder diffraction standards (JCPDS No. 19-629), shown in Fig. 4. With respect to the peaks of the spectrum, magnetic nanoparticles on the surface of WS have cubic crystal phase.

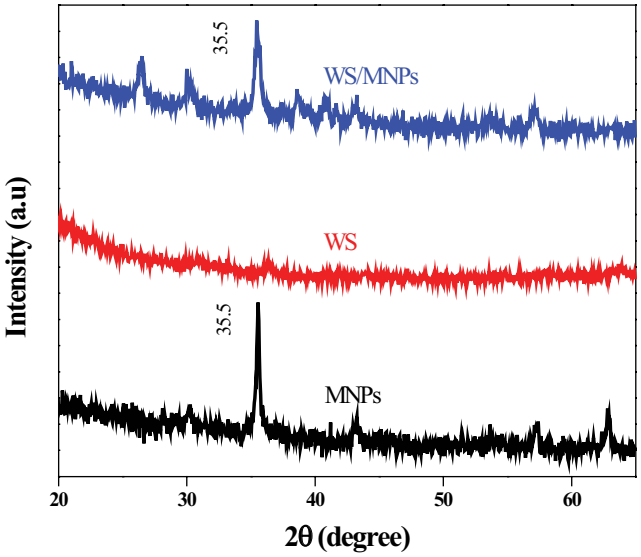

Fig. 4. XRD analysis for crystallinity of MNPs-WSP, MNPs and WSP.

3.2. Optimization studies

Different analytical parameters like, pH, vortex time, sample volume, temperature and initial metal ion concentration were optimized for quantitative recoveries of Cd(II) on MNP-WSP, MNPs and WSP. The percent recovery values were calculated by using the following equation:

$$\text{Recovery},\% = \left(\frac{w_o}{w_f}\times\right)100 \tag{4}$$

where w_o (μg) is the amount of analyte in final solution and w_f (μg) is the amount of analyte in sample solution, respectively

3.2.1. Effect of PH

pH is one of the most important parameter that significantly affect the adsorption capability. Preconcentration of Cd(II) was studied over pH range of 2–9 using MNPs-WSP, MNPs and WSP and % recovery results are shown in Fig. 5. It can be concluded from the Fig. 5 that % recovery of Cd(II) increases as pH of the solution increases from 2 to 7. Above pH 7 there is a significant decrease in % recovery of Cd(II) in case of MNPs-WSP and MNPs adsorbents. While in case of WSP maximum % recovery of Cd(II) was obtained at pH 8. It can be explained that as pH of the solution increases the interaction between negatively charged surface of the adsorbent and Cd(II) also increases, as a result % recovery increases. However, at low pH the hydrogen ion concentrations are high due to which most of the vacant sites of the adsorbent occupied by them and thus decrease

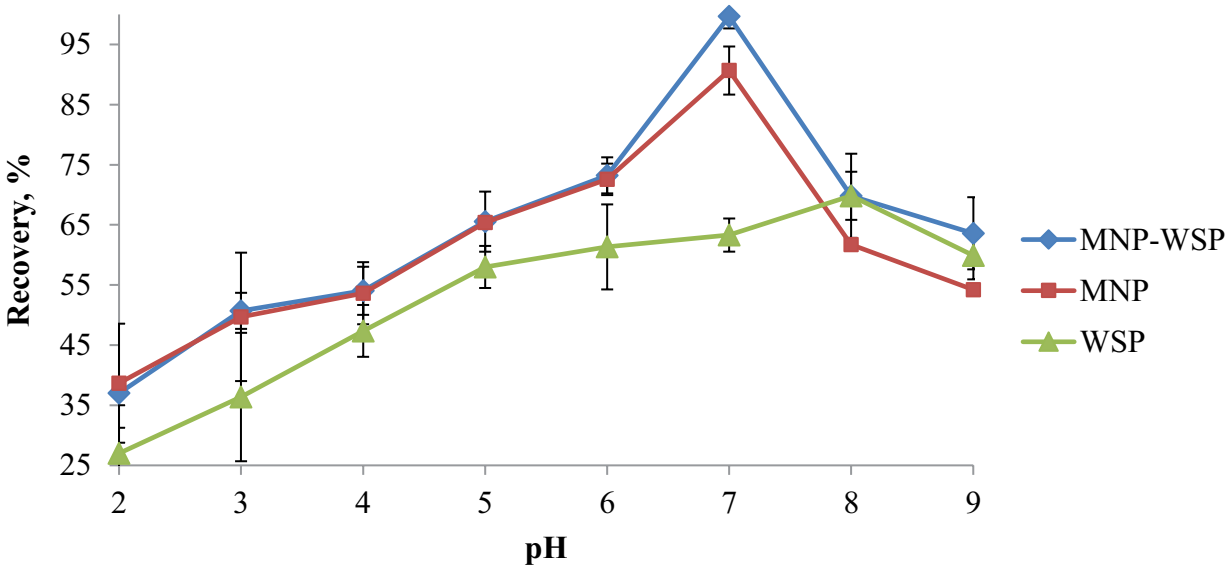

Fig. 5. Influence of pH on % recovery of Cd(II) using MNPs-WSP, MNPs and WSP (Volume of sample: 15 mL; amount of adsorbent: 0.1 g; final volume: 0.5 mL; $N = 3$).

the % recovery of Cd(II). In the range of pH 6 to 8 the surface of adsorbent is neutral and is suitable for quantitative % recovery of Cd(II). At higher pH metal hydroxide formation takes place that also decrease the % recovery of Cd(II). So the maximum recovery obtained at pH 7 on the surface of two adsorbents MNPs-WSP and MNPs, respectively. Therefore, pH 7 was the optimum pH which was maintain in other optimization studies.

3.2.2. Effect of sample volume

In order to achieve highest preconcentration factor the solid phase extraction studies were conducted at different sample volume ranging from 5–25 mL. Recovery results shown in Fig. 6 indicate that the proposed method can be successfully applied up to 20 mL of sample volume in case of MNPs-WSP and MNPs adsorbents. Above 20 mL there is significant decrease in the percent recoveries of Cd(II) on MNPs-WSP and MNPs adsorbents. While in case of WSP quantitative %recovery was obtained using 15 mL of sample volume. After that increasing sample volume decrease the percent recovery on WSP. Therefore, preconcentration factor of 40 was achieved using 20 mL of sample volume in case of MNPs-WSP and MNPs while in case of WSP PF of 30 was obtained.

3.2.3. Effect of time

In order to obtain equilibrium time, the % recovery of Cd(II) was determined at different vortex time ranging from 1 to 5 min as shown in Fig. 7. It can be concluded from Fig. 7 that % recoveries of Cd(II) increases as the time increases and equilibrium was established in 4 min with quantitative % recoveries of Cd(II) (96 ± 1, 93 ± 1 and 92 ± 1) on MNPs-WSP, MNPs and WSP, respectively. Therefore, 4 min of vortex time was used in further preconcentration studies.

3.2.4. Effect of temperature

SPE of Cd(II) on MNPs-WSP, MNPs and WSP was carried out at different temperatures ranging from 293 to 373 K as shown in Fig. 8. It can be concluded from Fig. 8 that % recoveries of Cd(II) increases as the temperature increases and equilibrium was established at 353 K with quantitative % recoveries of Cd(II) on MNPs-WSP, MNPs and WSP, respectively.

3.2.5. Effect of initial metal ion concentration

The effect of metal ion concentration on the adsorption capacities of Cd(II) from 0.1 g of MNPs-WSP, MNPs, and WSP were studied over the range of 1–5 ppm. The results illustrated in Fig. 9 show an obvious increase in the amount of metal ions Cd(II) retained in the solid phase, q_e, with an increase in their initial metallite concentrations within the investigated range. At low concentrations, metals are adsorbed by specific sites, while with increasing metal concentrations the specific sites are saturated and the exchange sites are filled [37]. These results may be ascribed to a sufficient capacity of MNPs-WSP, MNPs and WSP used to adsorb high concentrations of Cd(II) ions. The obtained results demonstrated that the maximum amount of metal ion retained in the MNPs-WSP. MNPs and WSP are 1.115, 1.096 and 1.048 mg g^{-1} for Cd(II) ions, respectively.

3.2.6. Kinetic studies

To evaluate the kinetic studies, pseudo-first-order and pseudo-second-order kinetics were employed to

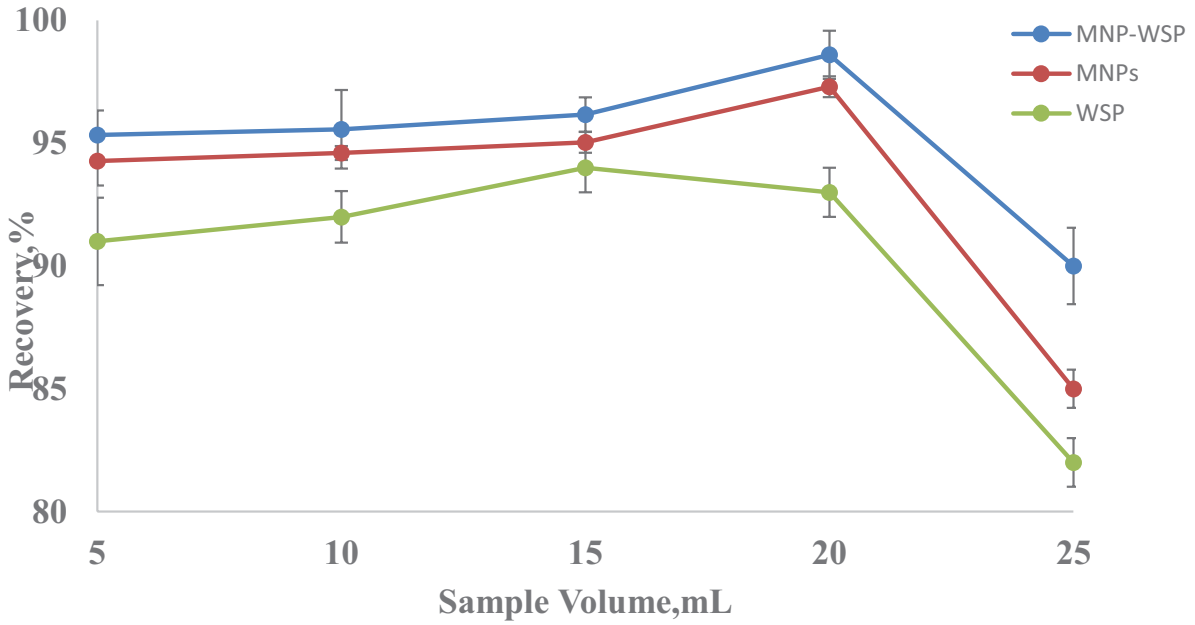

Fig. 6. Effect of sample volume on % recovery of Cd(II) using MNPs-WSP, MNPs and WSP (pH: 7; volume of sample: 15 mL; final volume: 0.5 mL; $N = 3$).

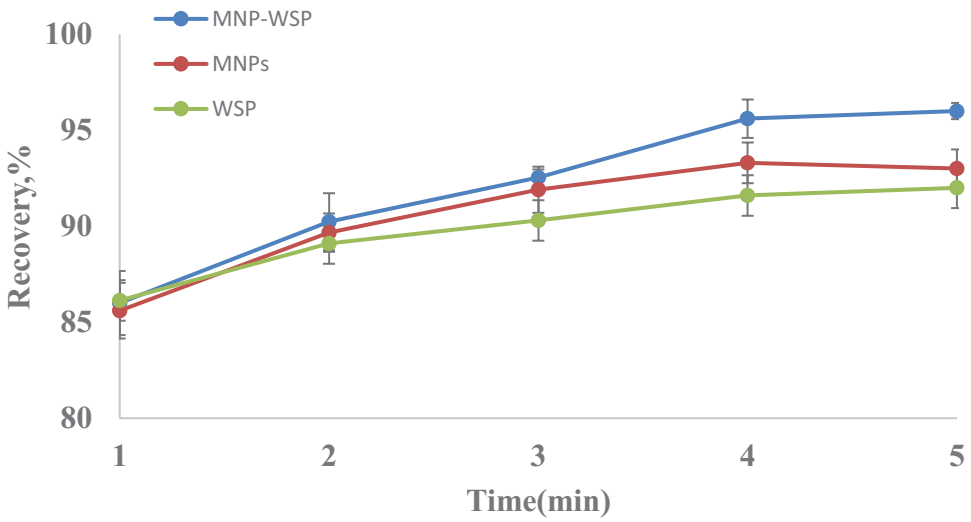

Fig. 7. Effect of time on % recovery of Cd(II) using MNPs-WSP, MNPs and WSP (pH: 7; volume of sample: 15 mL; final volume: 0.5 mL; $N = 3$).

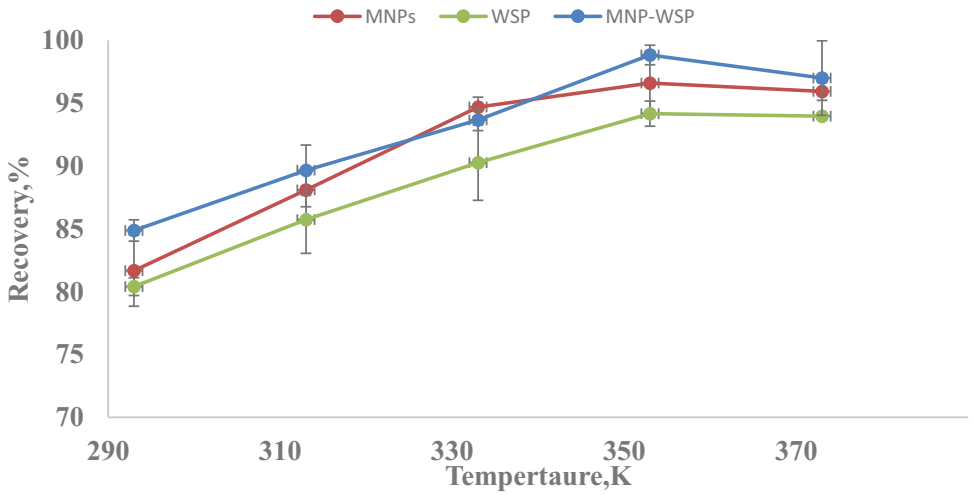

Fig. 8. Effect of temperature on % recovery of Cd(II) using MNPs-WSP, MNPs and WSP (pH: 7; volume of sample: 15 mL; final volume: 0.5 mL; $N = 3$).

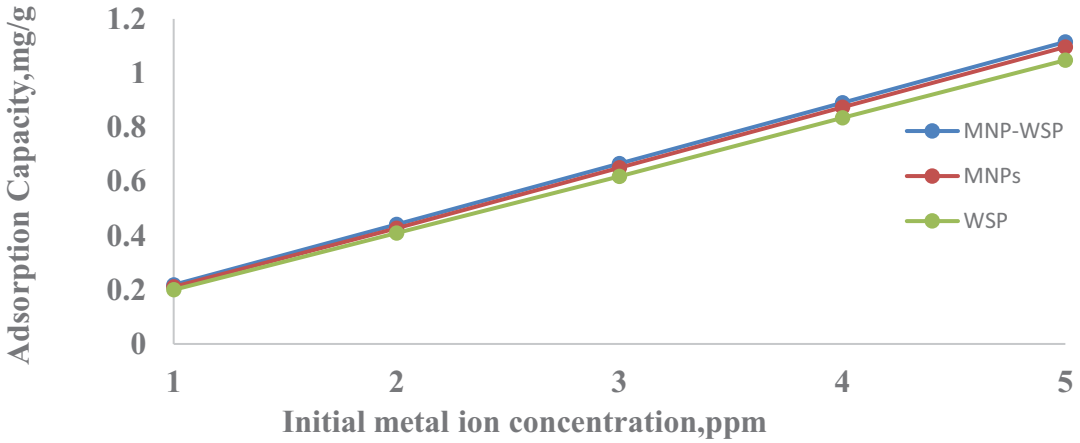

Fig. 9. Effect of initial metallite concentration on % recovery of Cd(II) using MNPs-WSP, MNPs and WSP (pH: 7; volume of sample: 15 mL; amount of adsorbent: 0.1 g; $N = 3$).

obtain useful information about adsorption efficiency of the adsorption of Cd(II) on MNPs-WSP, MNPs and WSP. For the pseudo-first-order kinetics the equation is given as under [38].

$$\log\left(q_e - q_t\right) = \log q_e - \frac{k_1}{2.303}t \tag{5}$$

where q_t and q_e are the adsorption capacities at time t (min) and at equilibrium time respectively and k_1 is the rate constant for pseudo-first-order kinetics of the adsorption process. The values of q_e and k_1 were calculated from the pseudo-first-order model and are given in Table 2. The calculated adsorption capacities from pseudo-first-order kinetics cannot coincide with experimental adsorption capacity. Therefore, the adsorption of Cd(II) on MNPs-WSP, MNPs and WSP cannot follow pseudo-first-order kinetics.

For the pseudo-second-order kinetics following equation is used [38].

$$\frac{t}{q_t} = \frac{t}{q_e} + \frac{1}{k_2 q_e^2} \tag{6}$$

where q_e and q_t are the sorption capacity at equilibrium and at time t, respectively; k_2 is rate constant for pseudo-second-order kinetics. The values of k_2 and q_e were calculated from pseudo-second-order model and are given in Table 2. The calculated adsorption capacities from pseudo-second-order kinetics are in close agreement with experimental adsorption capacities and the adsorption of Cd(II) on MNPs-WSP, MNPs and WSP follows pseudo-second-order kinetics.

3.2.7. Isotherm studies

Four adsorption isotherms Langmuir and Freundlich were applied to adsorption of Cd(II) on MNPs-WSP, MNPs and WSP to express adsorption equilibrium.

Monolayer adsorption on homogenous surfaces can be best explained by using Langmuir adsorption isotherm and linear form of the Langmuir adsorption isotherm is given as under [31].

$$\frac{C_e}{q_e} = \frac{1}{k_L} + \frac{a_L}{k_L}C_e \tag{7}$$

where q_e is the adsorption capacity in (mg g^{-1}), C_e is the equilibrium concentration of the metal ion in (mg L^{-1}), a_L and k_L are Langmuir constant related to the adsorption energy and adsorbate–adsorbent binding force respectively. The values of these parameters, correlation co-efficient (R^2) and the theoretical monolayer adsorption capacity ($Q°$) for the adsorption of Cd(II) on MNPs-WSP, MNPs and WSP were calculated and shown in Table 3.

The linear and non-linear form of Freundlich adsorption isotherm can be expressed by using the following two equation [39]. Freundlich adsorption isotherm is use to explain metal adsorption on heterogeneous surfaces.

$$q_e = k_F C_e^{1/n} \tag{8}$$

$$\log q_e = \log k_F + \frac{1}{n}\log C_e \tag{9}$$

where k_F is the relative adsorption capacity and $1/n$ indicates the intensity of adsorption process. The value of n, $1/n$, k_F and correlation coefficient (R^2) for the adsorption of Cd(II) on MNPs-WSP, MNPs and WSP were calculated and shown in Table 3.

3.2.8. Thermodynamic studies

For thermodynamic study the adsorption of Cd(II) on MNPs-WSP, MNPs and WSP were studied at different temperature. Various thermodynamic parameters like enthalpy

Table 3
Comparison of the parameters calculated from different isotherm models

Isotherm	Parameters	MNPs-WSP	MNPs	WSP
Freundlich	k_F (mg g^{-1})	1.16	0.805	0.675
	n	1.77	1.34	1.147
	$1/n$	0.5642	0.7462	0.8717
	R^2	0.9921	0.9988	0.9999
Langmuir	a_L (L mg^{-1})	2.33	0.625	0.24
	k_L (L g^{-1})	3,333.3	1,250	833.3
	$Q°$ (mg g^{-1})	1.43	2	3.47
	R^2	0.9015	0.9455	0.9145

Table 2
Different kinetic parameters for the adsorption of Cd(II) on MNPs-WSP, MNPs and WSP using different kinetic models

Kinetic model	Parameters	MNPs-WSP	MNPs	WSP
	$q_{e(exp)}$ (mg g^{-1})	0.215	0.194	0.187
Pseudo-first-order model	k_1 (min^{-1})	0.72	0.72	0.427
	q_e (mg g^{-1})	0.004	0.045	0.024
	R^2	0.815	0.671	0.321
Pseudo-second-order model	k_2 (min^{-1})	0.0007	0.02	0.058
	q_e (mg g^{-1})	0.222	0.204	0.185
	R^2	0.9996	0.9987	0.9963

($\Delta H°$), Gibbs free energy ($\Delta G°$) and entropy ($\Delta S°$) were calculated using the following equations [40].

$$K_D = \frac{q_e}{C_e} \tag{10}$$

$$\Delta G° = -RT \ln K_D \tag{11}$$

$$\Delta H° = R \frac{T_2 T_1}{T_2 - T_1} \ln \frac{K_2}{K_1} \tag{12}$$

$$\Delta S° = \frac{\Delta H° - \Delta G°}{T} \tag{13}$$

where K_D is the equilibrium constant, q_e and C_e are the equilibrium concentration of the metal ion on the adsorbent (mg L^{-1}) and the concentration of the metal ion in the solution (mg L^{-1}) respectively. It can be seen from Table 4, that the value of K_D increase with increase in temperature and also the value of $\Delta H°$ is positive which shows that the adsorption of Cd(II) on MNPs-WSP, MNPs and WSP is endothermic in nature. The positive values of $\Delta S°$ shows that these adsorption process is spontaneous in nature.

3.3. Matrix effect

The effect interfering ions that are coexisting ions with Cd(II) in the real water samples were carried out and the % recovery results are given in Table 5. It can be concluded from the results that the presence of these interfering ions has no significant effect on % recovery of Cd(II). This study shows that the method is highly selective.

3.4. Analytical performance of the method

All the analytical parameter like limit of detection (LOD), limit of quantification (LOQ), preconcentration factor (PF) and enhancement factor (EF) are given in the Table 6. All these parameters were calculated: The values of LOD were calculated as the ratio of three times standard deviation of ten blank absorbance's to the slope of the regression equation while the values of LOQ were calculated as ten times standard deviation of ten blank absorbance's to the slope of the regression equation. EF was calculated by using the ratio of the slops with and without the preconcentration step. PF was calculated as the ratio of the model solution to the final volume.

3.5. Application to the real sample

The proposed solid phase extraction method was applied for solid phase extraction of Cd(II) from tap water,

Table 6
Different analytical parameters of the method were calculated

Analytical parameters	MNPs-WSP	MNPs	WSP
Limit of detection (μg L^{-1})	0.69	0.37	1.64
Limit of quantification (μg L^{-1})	2.31	1.24	5.47
Preconcentration factor (PF)	40	40	30
Enhancement factor (EF)	40	40	30

Table 4
Thermodynamic parameter for the adsorption of Cd(II) on MNPs-WSP, MNPs and WSP

Temperature (K)	MNPs-WSP			MNPs			WSP		
	$\Delta G°$ (kJ mol^{-1})	$\Delta H°$ (kJ mol^{-1})	$\Delta S°$ (kJ mol^{-1})	$\Delta G°$ (kJ mol^{-1})	$\Delta H°$ (kJ mol^{-1})	$\Delta S°$ (kJ mol^{-1})	$\Delta G°$ (kJ mol^{-1})	$\Delta H°$ (kJ mol^{-1})	$\Delta S°$ (kJ mol^{-1})
293	–15.93			–15.23			–14.96		
313	–18.34			–17.87			–17.23		
333	–21.14	28.61	0.15	–21.69	24.15	0.13	–19.72	19.2	0.11
353	–27.70			–24.42			–22.68		
373	–26.22			–25.21			–23.85		

Table 5
Effect of interfering ions on % recoveries of Cd using MNPs-WSP, MNPs and WSP

Interfering ion	Added As	Concentration mg L^{-1}	MNPs-WSP	MNPs	WSP
Na^+	$NaNO_3$	1,000	98 ± 1	97 ± 2	90 ± 1
K^+	KCl	1,000	96 ± 2	96 ± 1	88 ± 1
Mg^{++}	$Mg(NO_3)_2{\cdot}6H_2O$	1,000	95 ± 1	99 ± 6	89 ± 3
Ca^{++}	$Ca(NO_3)_2{\cdot}4H_2O$	2,000	94 ± 1	99 ± 5	77 ± 1
F^-	NaF	500	97 ± 2	94 ± 2	91 ± 4
Ni	$Ni(NO_3)_2{\cdot}6H_2O$	50	96 ± 1	96 ± 2	90 ± 1
Pb	$Pb(NO_3)_2{\cdot}4H_2O$	50	96 ± 2	98 ± 2	87 ± 6

Table 7
Addition recovery result for removal of Cd(II) using MNPs-WSP, MNPs and WSP

Adsorbents	Sample	μg mL^{-1} added	μg mL^{-1} found	Recovery, %
MNPs-WSP	Wastewater	0	BDL	
		3	2.8	93 ± 10
		5	4.53	91 ± 7
	Dam water	0	BDL	
		3	2.56	86 ± 5
		5	4.33	87 ± 9
	Underground water	0	BDL	
		3	2.9	97 ± 6
		5	4.42	89 ± 10
	Tap water	0	BDL	
		3	2.95	98 ± 5
		5	4.25	85 ± 6
MNPs	Wastewater	0	BDL	
		3	2.9	96 ± 4
		5	4.56	91 ± 6
	Dam water	0	BDL	
		3	2.7	90 ± 3
		5	4.54	91 ± 6
	Underground water	0	BDL	
		3	2.79	93 ± 5
		5	4.29	86 ± 4
	Tap water	0	BDL	
		3	2.74	92 ± 6
		5	4.3	86 ± 2
WSP	Wastewater	0	BDL	
		3	2.8	93 ± 2
		5	4.49	90 ± 7
	Dam water	0	BDL	
		3	2.54	85 ± 1
		5	4.27	86 ± 5
	Underground water	0	BDL	
		3	2.84	95 ± 10
		5	4.49	90 ± 4
	Tap water	0	BDL	
		3	2.53	95 ± 10
		5	4.49	90 ± 4

dam water, wastewater and underground water samples and the % recovery results are given in Table 7. It can be concluded from Table 7 that all the % recovery results of Cd(II) are quantitative and the proposed solid phase extraction method can be successfully applied to the real water samples.

4. Conclusions

It can be concluded that:

- Magnetic solid phase extraction method for the preconcentration of Cd(II) using MNPs-WSP, MNPs and WSP as adsorbents was developed.
- The method is highly sensitive with low values of limit of detections 0.69, 0.37 and 1.64 μg L^{-1} for MNPs-WSP, MNPs and WSP respectively.
- Kinetic data fit to pseudo-second-order kinetics.
- Thermodynamic data shows that the method is feasible in nature.
- The Freundlich model better represented the equilibrium data.
- The method was successfully applied to environmental water samples like tap water, dam water, wastewater and underground water for addition recoveries.

References

[1] M.R. Shishehbore, A. Afkhami, H. Bagheri, Salicylic acid functionalized silica-coated magnetite nanoparticles for solid phase extraction and preconcentration of some heavy metal ions from various real samples, Chem. Cent. J., 5 (2011) 41, doi: 10.1186/1752-153X-5-41.
[2] X.-S. Wei, Y.-W. Wu, L.-J. Han, Determination of lead and cadmium in water and pharmaceutical products by inductively coupled plasma optical emission spectrometry with preconcentration by thiourea immobilized silica, Anal. Lett., 48 (2015) 996–1008.
[3] V. Gupta, A. Nayak, Cadmium removal and recovery from aqueous solutions by novel adsorbents prepared from orange peel and Fe_2O_3 nanoparticles, Chem. Eng. J., 180 (2012) 81–90.
[4] N.K. Srivastava, C.B. Majumder, Novel biofiltration methods for the treatment of heavy metals from industrial wastewater, J. Hazard. Mater., 151 (2008) 1–8.
[5] S. Nekouei, F. Nekouei, I. Tyagi, S. Agarwal, V.K. Gupta, Mixed cloud point/solid phase extraction of lead(II) and cadmium(II) in water samples using modified-ZnO nanopowders, Process Saf. Environ. Prot., 99 (2016) 175–185.
[6] M. Khan, J. Shah, M.R. Jan, Magnetic solid phase extraction of Cd(II) using magnetic nanoparticle (MNPs) and silica coated magnetic nanoparticles (SiMNPs) from environmental water samples, Desal. Water Treat., 83 (2017) 123–132.
[7] P. Liang, Y. Liu, L. Guo, J. Zeng, H.B. Lu, Multiwalled carbon nanotubes as solid-phase extraction adsorbent for the preconcentration of trace metal ions and their determination by inductively coupled plasma atomic emission spectrometry, J. Anal. At. Spectrom., 19 (2004) 1489–1492.
[8] N. Burham, S.A. Azeem, M.F. El-Shahat, Solid phase selective separation and green preconcentration of Cu, Zn, Pb and Cd in drinking water by using novel functionalized resin, Cent. Eur. J. Chem., 7 (2009) 945–954.
[9] U. Divrikli, A.A. Kartal, M. Soylak, L. Elci, Preconcentration of Pb(II), Cr(III), Cu(II), Ni(II) and Cd(II) ions in environmental samples by membrane filtration prior to their flame atomic absorption spectrometric determinations, J. Hazard. Mater., 145 (2007) 459–464.
[10] Y. Zhai, Q. He, Q. Han, Solid-phase extraction of trace metal ions with magnetic nanoparticles modified with 2,6-diaminopyridine, Microchim. Acta, 178 (2012) 405–412.
[11] M. Soylak, Z. Topalak, Multiwalled carbon nanotube impregnated with tartrazine: solid phase extractant for Cd(II) and Pb(II), J. Ind. Eng. Chem., 20 (2014) 581–585.
[12] A. Duran, M. Tuzen, M. Soylak, Preconcentration of some trace elements via using multiwalled carbon nanotubes as solid phase extraction adsorbent, J. Hazard. Mater., 169 (2009) 466–471.
[13] F. Xie, X. Lin, X. Wu, Z. Xie, Solid phase extraction of lead (II), copper (II), cadmium (II) and nickel (II) using gallic acid-modified silica gel prior to determination by flame atomic absorption spectrometry, Talanta, 74 (2008) 836–843.
[14] M. Khan, M. Soylak, Supramolecular solvent based liquid–liquid microextraction of aluminum from water and hair samples prior to UV-visible spectrophotometric detection, RSC Adv., 5 (2015) 62433–62438.

[15] F. Rezaei, Y. Yamini, M. Moradi, A comparison between emulsification of reverse micelle-based supramolecular solvent and solidification of vesicle-based supramolecular solvent for the microextraction of triazines, J. Chromatogr. A, 1327 (2014) 155–159.
[16] C. Baggiani, L. Anfossi, C. Giovannoli, Solid phase extraction of food contaminants using molecular imprinted polymers, Anal. Chim. Acta, 591 (2007) 29–39.
[17] L. Guo, X. Ma, X. Xie, R. Huang, M. Zhang, J. Li, G. Zeng, Y. Fan, Preparation of dual-dummy-template molecularly imprinted polymers coated magnetic graphene oxide for separation and enrichment of phthalate esters in water, Chem. Eng. J, 361 (2019) 245–255.
[18] N. AlMasoud, S.M. Wabaidur, Z.A. Alothman, A.A. Ghfar, T.S. Alomar, A solid phase extraction based UPLC-ESI-MS/MS method using surfactant-modified clay as extraction sorbent for the removal and determination of rhodamine B in industrial wastewater samples, Desal. Water Treat., 195 (2020) 222–231.
[19] H.İ. Ulusoy, A versatile hydrogel including bentonite and gallocyanine for trace Rhodamine B analysis, Colloids Surf., A, 513 (2017) 110–116.
[20] K. Kadirvelu, C. Namasivayam, Activated carbon from coconut coirpith as metal adsorbent: adsorption of Cd(II) from aqueous solution, Adv. Environ. Res., 7 (2003) 471–478.
[21] M. Iqbal, A. Saeed, S.I. Zafar, FTIR spectrophotometry, kinetics and adsorption isotherms modeling, ion exchange, and EDX analysis for understanding the mechanism of Cd^{2+} and Pb^{2+} removal by mango peel waste, J. Hazard. Mater., 164 (2009) 161–171.
[22] J. Shah, M.R. Jan, M. Khan, S. Amir, Removal and recovery of cadmium from aqueous solutions using magnetic nanoparticle-modified sawdust: kinetics and adsorption isotherm studies, Desal. Water Treat., 57 (2016) 9736–9744.
[23] W. Aeungmaitrepirom, W. Ngeontae, T. Tuntulani, Silica gel chemically modified with ethyl-2-benzothiazolylacetate for selective extraction of Pb(II) and Cu(II) from real water samples, Anal. Sci., 25 (2009) 1477–1482.
[24] L. Elci, A.A. Kartal, M. Soylak, Solid phase extraction method for the determination of iron, lead and chromium by atomic absorption spectrometry using Amberite XAD-2000 column in various water samples, J. Hazard. Mater., 153 (2008) 454–461.
[25] R. Huang, X. Ma, X. Li, L. Guo, X. Xie, M. Zhang, J. Li, A novel ion-imprinted polymer based on graphene oxide-mesoporous silica nanosheet for fast and efficient removal of chromium (VI) from aqueous solution, J. Colloid Interface Sci., 514 (2018) 544–553.
[26] M. Zhang, B.L. Cushing, C.J. O'Connor, Synthesis and characterization of monodisperse ultra-thin silica-coated magnetic nanoparticles, Nanotechnology, 19 (2008) 085601, doi: 10.1088/0957-4484/19/8/085601.
[27] X. Xie, X. Ma, L. Guo, Y. Fan, G. Zeng, M. Zhang, J. Li, Novel magnetic multi-templates molecularly imprinted polymer for selective and rapid removal and detection of alkylphenols in water, Chem. Eng. J., 357 (2019) 56–65.
[28] J. Hu, G. Chen, I.M. Lo, Removal and recovery of Cr(VI) from wastewater by maghemite nanoparticles, Water Res., 39 (2005) 4528–4536.
[29] Y. Shen, J. Tang, Z. Nie, Y. Wang, Y. Ren, L. Zuo, Preparation and application of magnetic Fe_3O_4 nanoparticles for wastewater purification, Sep. Purif. Technol., 68 (2009) 312–319.
[30] J.-f. Liu, Z.-s. Zhao, G.-b. Jiang, Coating Fe_3O_4 magnetic nanoparticles with humic acid for high efficient removal of heavy metals in water, Environ. Sci. Technol., 42 (2008) 6949–6954.
[31] S.H. Huang, D.H. Chen, Rapid removal of heavy metal cations and anions from aqueous solutions by an amino-functionalized magnetic nano-adsorbent, J. Hazard. Mater., 163 (2009) 174–179.
[32] S.S. Banerjee, D.H. Chen, Fast removal of copper ions by gum arabic modified magnetic nano-adsorbent, J. Hazard. Mater., 147 (2007) 792–799.
[33] A. Badruddoza, A. Tay, P. Tan, K. Hidajat, M. Uddin, Carboxymethyl-β-cyclodextrin conjugated magnetic nanoparticles as nano-adsorbents for removal of copper ions: synthesis and adsorption studies, J. Hazard. Mater., 185 (2011) 1177–1186.
[34] Y. Zhai, Q. He, X. Yang, Q. Han, Solid phase extraction and preconcentration of trace mercury(II) from aqueous solution using magnetic nanoparticles doped with 1, 5-diphenylcarbazide, Microchim. Acta, 169 (3010) 353–360.
[35] J. Li, X. Zhao, Y. Shi, Y. Cai, S. Mou, G. Jiang, Mixed hemimicelles solid-phase extraction based on cetyltrimethylammonium bromide-coated nano-magnets Fe_3O_4 for the determination of chlorophenols in environmental water samples coupled with liquid chromatography/spectrophotometry detection, J. Chromatogr. A, 1180 (2008) 24–31.
[36] Y.-H. Deng, C.-C. Wang, J.-H. Hu, W.-L. Yang, S.-K. Fu, Investigation of formation of silica-coated magnetite nanoparticles via sol–gel approach, Colloids Surf., A, 262 (2005) 87–93.
[37] J. Shah, M.R. Jan, A. ul Haq, Removal of lead from aqueous media using carbonized and acid treated orange peel, Tenside, Surfactants, Deterg., 51 (2013) 240–246.
[38] Z. Reddad, C. Gerente, Y. Andres, P. Le Cloirec, Adsorption of several metal ions onto a low-cost biosorbent: kinetic and equilibrium studies, Environ. Sci. Technol., 36 (2002) 2067–2073.
[39] N. Atar, A. Olgun, S. Wang, Adsorption of cadmium (II) and zinc (II) on boron enrichment process waste in aqueous solutions: batch and fixed-bed system studies, Chem. Eng. J., 192 (2012) 1–7.
[40] V.K. Gupta, C.K. Jain, I. Ali, M. Sharma, V.K. Saini, Removal of cadmium and nickel from wastewater using bagasse fly ash—a sugar industry waste, Water Res., 37 (2003) 4038–4044.